A Comparative Study of 4500V Edge Termination Techniques for SiC Devices

Woongje Sung, *Member, IEEE*, B. J. Baliga, *Life Fellow, IEEE*

***Abstract*— This paper compares five edge termination techniques for SiC high voltage devices: Single Zone Junction Termination Extension (SZ-JTE), Ring Assisted-JTE (RA-JTE), Multiple Floating Zone-JTE (MFZ-JTE), Hybrid-JTE, and Floating Field Rings (FFRs). PiN diodes with these edge terminations were fabricated on a 4.5kV-rated 4H-SiC epi-layer. It was experimentally demonstrated that the Hybrid-JTE provides a nearly ideal breakdown voltage (~99% of the ideal parallel plane breakdown voltage) with a stable avalanche blocking behavior. RA-JTE, with tight control of the JTE implant dose, is demonstrated to be the most area-efficient edge termination structure for SiC power devices.**

***Index Terms*—Silicon Carbide, 4H-SiC, Edge termination, Junction Termination Extension, JTE, Floating Field Ring, Guard Ring**

I. Introduction

High critical electric field of 4H-Silicon Carbide (4H-SiC) allows the voltage sustaining drift-layer of a power device to be designed thin and highly conductive, and therefore provides a low on-resistance. In order to fully exploit this benefit while keeping the breakdown voltage close to the ideal value that is determined by the material property, an efficient edge termination technique becomes the most critical aspect in developing power devices on 4H-SiC [1]. Floating field rings (FFRs) [2] and junction termination extension (JTE) and its modified forms [3-9] have been widely used as edge termination structures for 4H-SiC high voltage devices. The FFR method is attractive because it can be formed with the p+ main junction in PiN and JBS diodes or the p+ body contact region in the power MOSFET [1]. However, the FFRs generally require fine patterning and etching processes to define narrow spaces between the p+ concentric rings. Single Zone JTE (SZ-JTE) is simple but, very sensitive to the implant dose. Ring assisted JTE (RA-JTE) [5], multiple floating zone JTE (MFZ-JTE) [6], space modulated JTE (SM-JTE) [7] have been proposed to widen the process latitude. Recently, the Hybrid-JTE that combines RA-JTE and MFZ-JTE was proposed to further improve the breakdown voltage over a wide range of implant doses [8, 9].

This paper reports a comparative study of the aforementioned edge termination techniques for 4H-SiC devices, for the first time. 4500V-rated PiN diodes using various edge termination structures were fabricated and compared with regard to breakdown voltage efficiency, area consumption, process yield, and avalanche ruggedness. Detailed experimental results from PiN diodes using five edge termination techniques with two different implant doses on 16- randomly chosen dies are provided in this paper.

II. Design of The Proposed Edge Termination Structrures

Fig. 1 shows simplified cross-sectional views of PiN diodes with various edge termination structures. Optimized designs based on extensive device simulations and the resulting total widths used for each edge termination approach are summarized in Table1. A 40μm thick-, 2×10^{15}cm^{-3} doped drift layer was chosen to attain 5500V from the parallel plane p+n diode [1]. Fig. 1(a) depicts the 35-FFRs design. FFRs should be designed to reduce the electric field enhancement at the main junction by locating the rings tightly near the main junction. More space must be allocated for the outer rings so that they can share the voltage uniformly enabling reduction of the electric field at the last ring. The spacing between each ring is gradually increased in a manner that $S_n=S_1+(n-1)\times S_i$, where S_1 is the first spacing, and S_i is the incremental spacing. The optimized first spacing was found to be S_1=0.6μm, and the incremental spacing was found to be S_i=0.08μm. The optimized first spacing is narrower than the critical dimension (0.8μm) of our photolithography tool such that the first two spacing were compromised to 0.8μm. The simulated breakdown voltage with optimized 35-rings was 4570V. The electric field distribution at the breakdown condition is also shown in the inset of Fig 1(a). Electric fields at the main junction and at the last ring are well suppressed with the optimized FFR design. 35-and 45-FFRs having the same design parameters were included in the mask set.

Manuscript received November xx, 2016. The information, data, or work presented herein was funded in part by the Office of Energy Efficiency and Renewable Energy (EERE), U.S. Department of Energy, under Award Number DE-EE0006521 with North Carolina State University, PowerAmerica Institute.

The information, data, or work presented herein was funded in part by an agency of the United States Government. Neither the United States Government nor any agency thereof, nor any of their employees, makes any warranty, express or implied, or assumes any legal liability or responsibility for the accuracy, completeness, or usefulness of any information, apparatus, product, or process disclosed, or represents that its use would not infringe privately owned rights. Reference herein to any specific commercial product, process, or service by trade name, trademark, manufacturer, or otherwise does not necessarily constitute or imply its endorsement, recommendation, or favoring by the United States Government or any agency thereof. The views and opinions of authors expressed herein do not necessarily state or reflect those of the United States Government or any agency thereof.

W. Sung is with Colleges of Nanoscale Science and Engineering, State University of New York Polytechnic Institute, Albany, NY 12203, USA (e-mail: wsung@sunypoly.edu).

B. J. Baliga is with PowerAmerica Institute, North Carolina State University, Raleigh, NC 27695, USA.

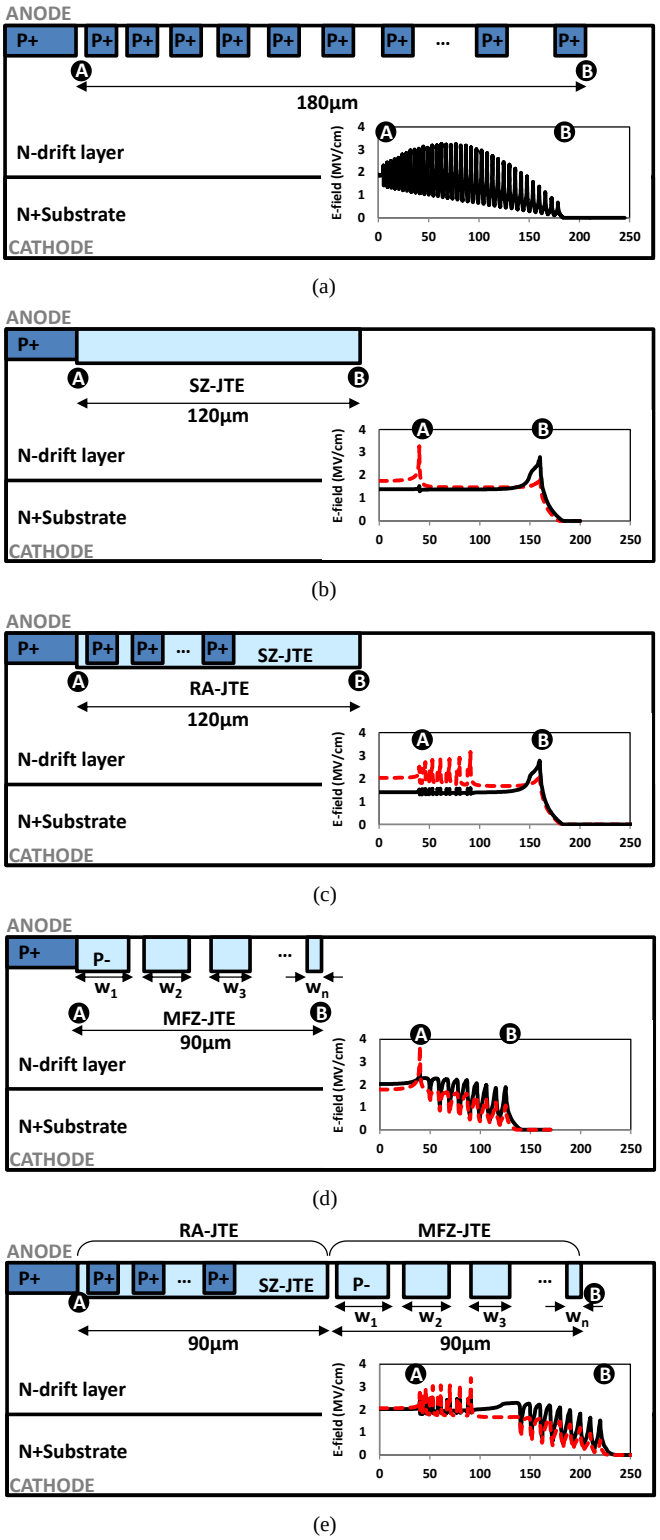

Fig. 1. Cross-sectional view of (a) Floating Field Rings (FFRs), (b) Single Zone JTE (SZ-JTE), (c) Ring Assisted JTE (RA-JTE), (d) Multiple Floating Zone JTE (MFZ-JTE), and (e) Hybrid-JTE. Simulated electric fields at the junction depth are shown in the insets of each structure. For the case of JTE-based edge termination structures, red dashed line indicates the low dose case (9×10^{12}cm^{-2}) and solid black line shows the high dose (1.25×10^{13}cm^{-2}) case.

Fig. 1(b) shows the single zone JTE (SZ-JTE) structure. The most critical parameter in designing a SZ-JTE is the charge in the JTE region. With a smaller charge in the JTE region than the optimum one, little impact on the electric field distribution is expected, whereas JTE with high dose merely serves as an extension of the main junction [1]. As shown in Fig. 2, there is a sharp peak of breakdown voltage with the optimized dose of 1×10^{13}cm^{-2}. Electric fields at the junction depth with doses 9×10^{12}cm^{-2} and 1.25×10^{13}cm^{-2} are depicted in the insets of Fig. 1(b)-(e). It should be noted that it is difficult to attain stable breakdown voltages using the SZ-JTE because of the narrow process latitude.

Table 1. Fabricated PiN diodes with proposed edge termination structures

Device ID	Design description
FFR_35R_180µm	35-rings, W=3µm, S_1=0.8µm, S_i=0.08µm, Total width=180µm
FFR_45R_250µm	45-rings, W=3µm, S_1=0.8µm, S_i=0.08µm, Total width=250µm
SZ-JTE_120µm	W_{jte}=120µm
SZ-JTE_200µm	W_{jte}=200µm
RA-JTE_120µm	W_{jte}=120µm, Ring design: 6-rings, W=3µm, S_1=3µm, S_i=1µm
RA-JTE_200µm	W_{jte}=200µm, Ring design: 6-rings, W=3µm, S_1=3µm, S_i=1µm
MFZ-JTE_90µm	W_{jte}=90µm, 9-zone, α=1.07
MFZ-JTE_120µm	W_{jte}=120µm, 12-zone, α=1.05
Hybrid_180µm	RA-JTE_90µm + MFZ-JTE_90µm
Hybrid_240µm	RA-JTE_120µm + MFZ-JTE_120µm

In the ring assisted JTE (RA-JTE) method, floating field rings are inserted in the SZ-JTE, as shown in Fig. 1(c) in order to relieve the electric field crowding near the main junction. 6-concentric rings were placed in our SZ-JTE design. Each ring was 3 µm wide, and placed using the same methodology used in the design of the FFRs. The optimized RA-JTE design has S_1=3 µm, and S_i=1µm. It is noteworthy that the spacing between rings for the case of RA-JTE is much wider than that for FFRs, which is favored from the manufacturability perspective. The RA-JTE prevents enhancement of the electric field at a lower dose than the optimum JTE dose for the SZ-JTE as shown in the inset of Fig. 1(c). As a result, RA-JTE provides higher breakdown voltages at lower doses than the SZ-JTE as shown in Fig. 2. It is known that the width of JTE-based edge termination structures should be sufficient in order to guarantee reliable blocking performances. It has been reported that the JTE width needs to be at least 3 times larger than the drift region thickness [10]. Consequently, SZ-JTE and RA-JTE designs with 3-times and 5-times the drift layer thickness (40 µm) were fabricated.

A high dose in the SZ-JTE and the RA-JTE structures produces a high e-field at the outer edge of the JTE region as shown in Fig. 1(b) and 1(c) which drastically reduces the breakdown voltage as shown in Fig. 2. In contrast, the multiple floating zone JTE (MFZ-JTE) method has been experimentally proven to be effective for achieving high breakdown voltages at high JTE doses [6]. In the MFZ-JTE, a gradual charge distribution is achieved by controlling the width of the discrete implanted regions: $W_n=W_1/\alpha(n-1)$. The width of discrete charge zone (W_n) is decreased by parameter α. In our design, α of 1.07 was found to be the optimum value for a 10-zone MFZ-JTE design with total width of 90 µm. A separately optimized, 120µm-wide MFZ-JTE was also included in the experiment.

After individually optimizing the RA-JTE and MFZ-JTE designs, the Hybrid-JTE can be constructed by simply placing

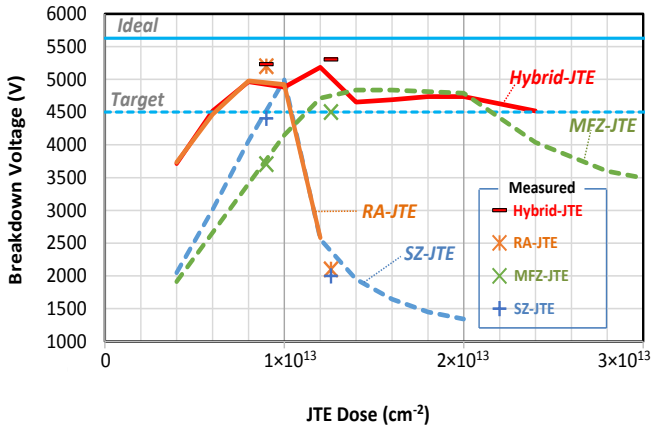

Fig. 2 Simulated breakdown voltages of SZ-JTE, RA-JTE, MFZ-JTE, and Hybrid-JTE. Measured breakdown voltages are indicated by markers. It is important to note that the actual charges in JTE regions are lower than the implanted doses (1.3×10^{13}cm^{-2} and 1.8×10^{13}cm^{-2}) due to the incomplete activation. Assuming about 70% activation rate, measured breakdown voltages (shown by markers at 9×10^{12}cm^{-2} and 1.25×10^{13}cm^{-2}) are well matched with simulated values.

the RA-JTE near the P+ main junction, and the MFZ-JTE next to the RA-JTE as shown in Fig. 1(e). In this way, the electric field can be more uniformly distributed for a wider range of doses without having crowded electric fields at either the main junction or the edge of the JTE. As shown in Fig. 2, the superposition of simulated breakdown voltages of the RA-JTE and MFZ-JTE matches with the simulated breakdown voltage for the Hybrid-JTE. The total widths used for the Hybrid-JTE in this study are 180µm and 240µm (4.5-times and 6-times the drift layer thickness, respectively).

III. Experimental Results and Discussions

A 40µm thick, 2×10^{15}cm^{-3} doped n-type epitaxial layer on a 6-inch, n+ 4H-SiC substrate was used to fabricate PiN diodes terminated with the five edge termination structures. The P+ main junction and FFRs were formed by aluminum implants with a total dose of 1×10^{15}cm^{-2} and a maximum energy of 150keV. The JTE regions were formed by aluminum ion implantation with two different total doses. The implant doses used in the JTE designs were 1.3×10^{13}cm^{-2}, and 1.8×10^{13}cm^{-2}. The implantation steps were followed by a 1650℃, 10min activation anneal with a carbon cap. An interlayer dielectric was deposited and etched to open the contact to the P+ main junction. Ni was deposited on the frontside and patterned, followed by a RTA step. Backside metal contact was also formed by Ni and the same RTA process. 4µm thick Al-based metal was deposited and patterned to complete the anode metal. Frontside was passivated by nitride and polyimide. Fig. 3 shows the picture of the fully processed 6-inch wafer with location of the dies that were characterized in this study.

Fig. 4, 5, 6, 7, and 8 summarize reverse blocking characteristics of fabricated PiN diodes with FFRs, SZ-JTE, RA-JTE, MFZ-JTE, and Hybrid-JTE, respectively. JTE-based edge terminations received total JTE dose of 1.3×10^{13}cm^{-2} in these cases. For both the RA-JTE and the Hybrid-JTE, the measured breakdown voltage is as high as 5400V at anode

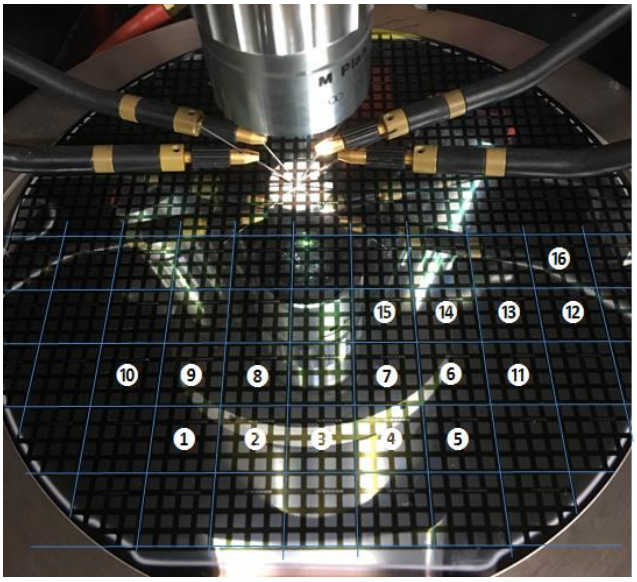

Fig. 3. Picture of the 6-inch wafer after the full process completed. Each die possesses PiN diodes that are terminated with SZ-, RA-, MFZ-, Hybrid-JTE, and FFRs. Die number 1 – 16 were measured and characterized. Dies were randomly selected.

current of 100µA, which is 99% of the ideal value for a 1-D structure calculated using Konstantinov's form for the critical electric field [11] for our structure [1]. The SZ-JTE and MFZ-JTE showed lower breakdown voltages because the JTE implant dose is lower than the optimum value for them as discussed in the previous section. The breakdown voltage of MFZ-JTE increases to over 4500V with a dose of 1.8×10^{13}cm^{-2}. This does not happen with the SZ-JTE. Simulated and measured breakdown voltages of the JTE-based edge termination structures are compared in Fig. 2. The measured breakdown voltages are well matched with the simulated values if 70% activation efficiency is assumed for the aluminum JTE implants. The maximum breakdown voltage from the PiN diode with FFRs was 4160V. Furthermore, a significant increase in leakage current is observed at relatively low voltage (~2000V) for the FFR case. In contrast, PiN diodes with JTE-based edge termination structures exhibit very low reverse leakage currents until voltages close to the breakdown condition.

Comparison of breakdown voltages of two different sizes for the same kind of edge termination techniques is shown in Fig. 4-8 (c). The breakdown voltage increases by only about 2.5% for the case of FFRs and the SZ-JTE with increased width. It can be concluded that no significant improvement in breakdown voltages is observed by using a larger area for these edge terminations. The geographical trends in breakdown voltage from two versions (different widths) of the same edge termination technique are very similar, which suggests the measured breakdown voltages show the maximum capability of the corresponding edge termination technique. It can be concluded that the breakdown voltages are governed by the material parameters namely the doping concentration and thickness of the drift layer. The RA-JTE and the Hybrid-JTE show almost identical geographical trends in breakdown voltages because the blocking characteristics of the Hybrid-JTE at a low JTE dose is solely determined by the RA-JTE portion in

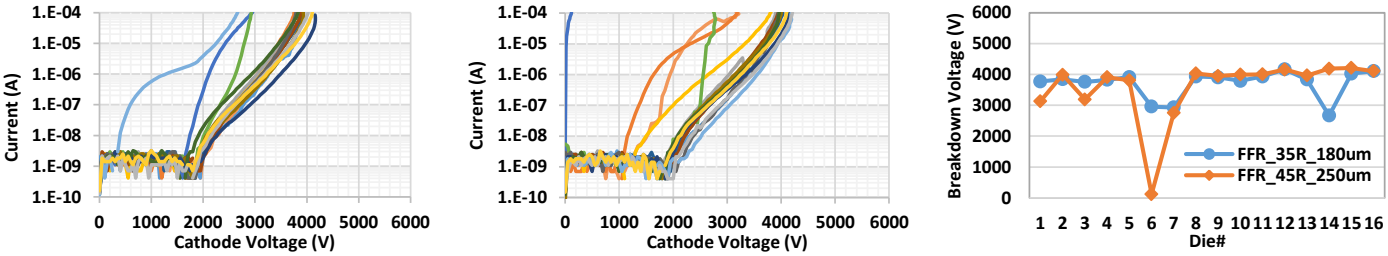

(a) FFR_35R_180µm (b) FFR_45R_250µm (c) Breakdown voltages at 100µA

Fig. 4. Reverse blocking characteristics of (a) FFR_35R_180µm (b) FFR_45R_250µm, and (c) their comparison

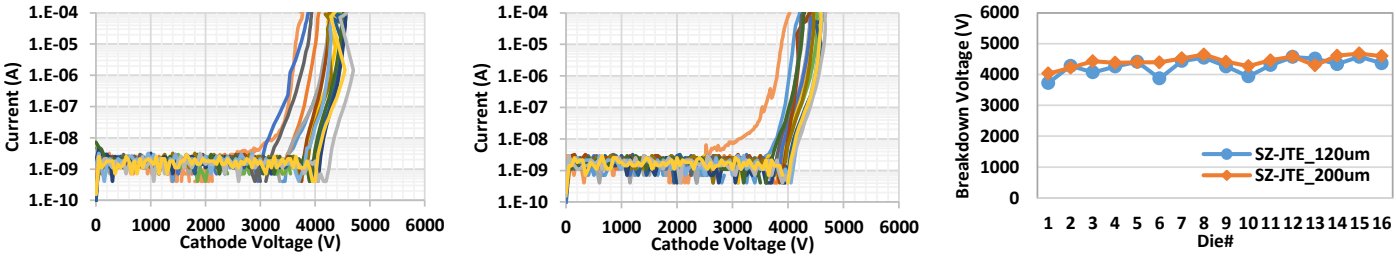

(a) SZ-JTE_120µm (JTE dose=1.3×10^{13}cm^{-2}) (b) SZ-JTE_200µm (JTE dose=1.3×10^{13}cm^{-2}) (c) Breakdown voltages at 100µA

Fig. 5. Reverse blocking characteristics of (a) SZ-JTE_120µm (b) SZ-JTE_200µm, and (c) their comparison

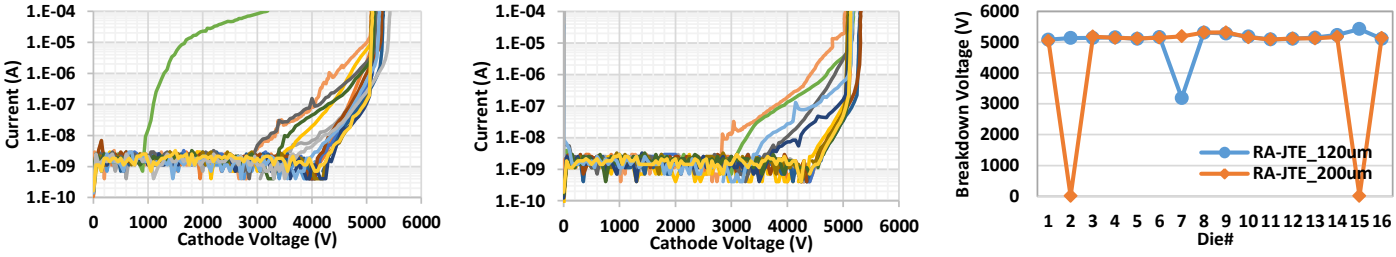

(a) RA-JTE_120µm (JTE dose=1.3×10^{13}cm^{-2}) (b) RA-JTE_200µm (JTE dose=1.3×10^{13}cm^{-2}) (c) Breakdown voltages at 100µA

Fig. 6. Reverse blocking characteristics of (a) RA-JTE_120µm (b) RA-JTE_200µm, and (c) their comparison

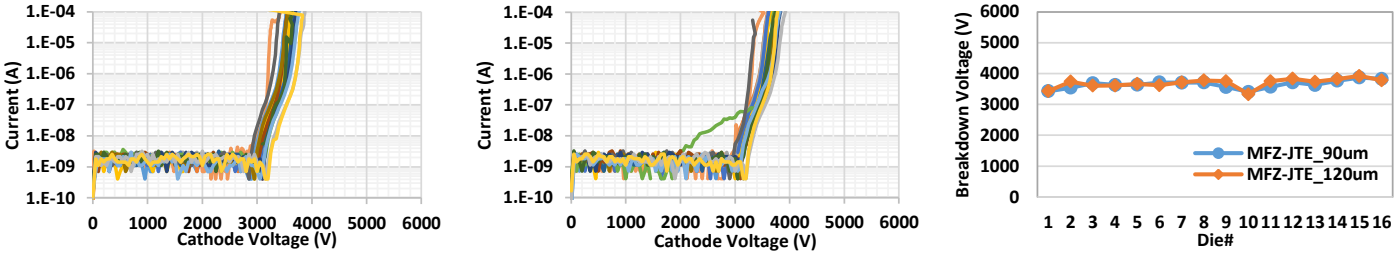

(a) MFZ-JTE_90µm (JTE dose=1.3×10^{13}cm^{-2}) (b) MFZ-JTE_120µm (JTE dose=1.3×10^{13}cm^{-2}) (c) Breakdown voltages at 100µA

Fig. 7. Reverse blocking characteristics of (a) MFZ-JTE_90µm (b) MFZ-JTE_120µm, and (c) their comparison

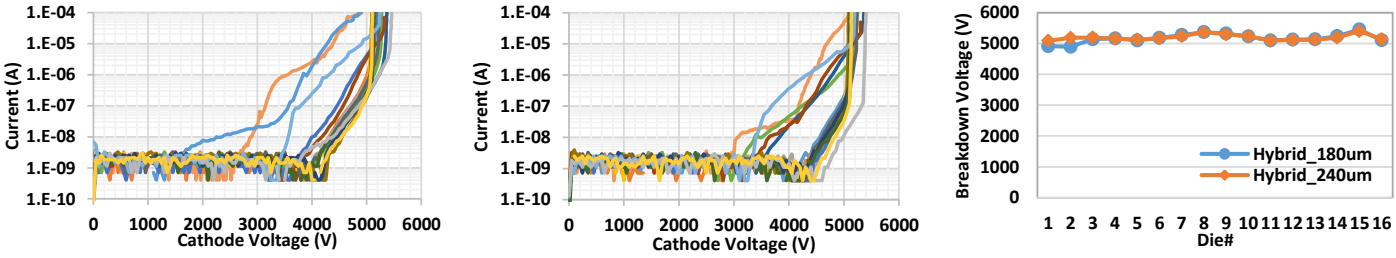

(a) Hybrid_180µm (JTE dose=1.3×10^{13}cm^{-2}) (b) Hybrid_240µm (JTE dose=1.3×10^{13}cm^{-2}) (c) Breakdown voltages at 100µA

Fig. 8. Reverse blocking characteristics of (a) Hybrid_180µm (b) Hybrid_240µm, and (c) their comparison

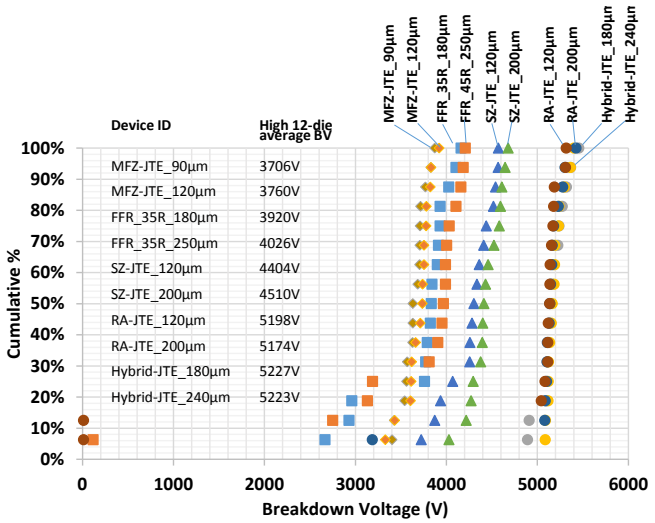

Fig. 9. Cumulative distribution of breakdown voltages measured from randomly chosen 16 dies with different edge termination structures. Breakdown voltages were read at 100 µA.

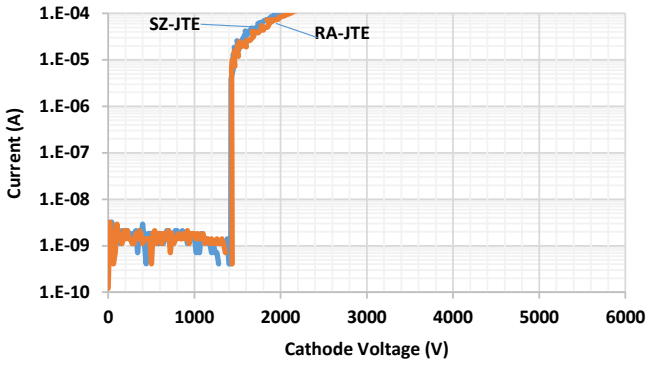

Fig. 10. Typical reverse blocking characteristics of PiN diodes using the SZ-JTE and the RA-JTE when the JTE implant dose is 1.8×10^{13}cm^{-2}.

its structure as described in the previous section. Likewise, the SZ-JTE and the MFZ-JTE are similar in the operation mechanism at a low JTE dose resulting in similar trends on different dies. These behaviors are consistent with the electric field distributions in each structure as depicted in Fig. 1.

It is very important to investigate the distribution of measured breakdown voltages for a high yield of good dies and thus to reduce the chip cost. Fig. 9 compares the cumulative distributions of breakdown voltages measured on PiN diodes with the proposed edge termination structures. As shown, both RA-JTE and the Hybrid-JTE show very tight distribution; 59ea out of total 64 devices (92%) accomplished >5000V. The RA-JTE and the Hybrid-JTE achieved approximately 700V higher breakdown voltages in average compared with SZ-JTEs. This is a significant improvement in that it was achieved by simple additions of p+ concentric rings without any additional processes or a fine lithography process.

However, at a higher JTE dose (1.8×10^{13}cm^{-2}), RA-JTE produces very low breakdown voltages as shown in Fig. 10. As explained earlier, the SZ-JTE has electric field enhancement at the edge of its structure at a higher JTE dose than the optimum value. The measured breakdown voltages are well matched with the simulated value as shown in Fig. 2.

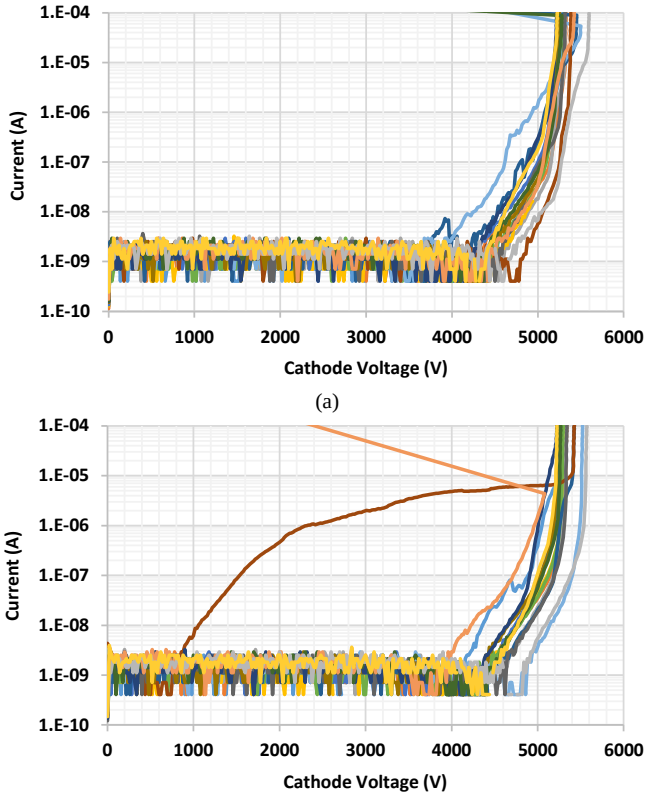

Fig. 11. Reverse blocking characteristics of PiN diodes using the (a) Hybrid-JTE_180µm and (b) Hybrid-JTE_240µm when the JTE implant dose is 1.8×10^{13}cm^{-2}.

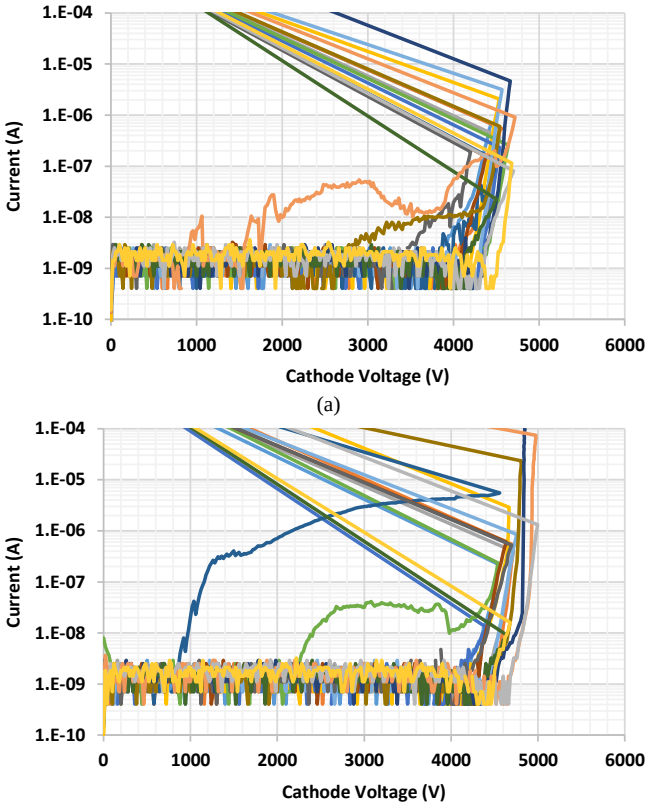

Fig. 12. Reverse blocking characteristics of PiN diodes using the (a) MFZ-JTE_90µm and (b) Hybrid-JTE_120µm when the JTE implant dose is 1.8×10^{13}cm^{-2}.

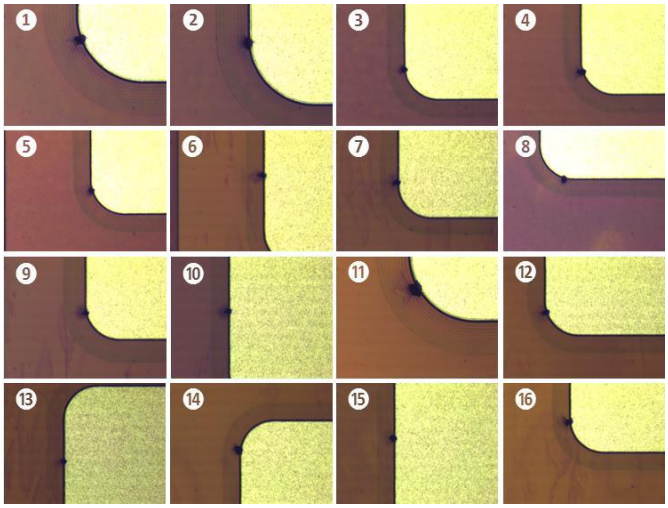

(a)

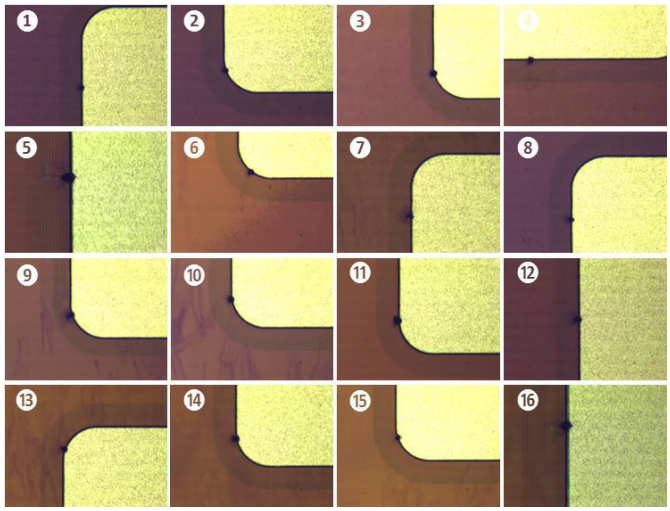

(b)

Fig. 13. Microscopic images of failures after measurements of reverse blocking characteristics of PiN diodes with the (a) MFZ-JTE_90µm and (b) Hybrid-JTE_120µm when the JTE implant dose is 1.8×10^{13}cm^{-2}.

The reverse blocking characteristics of the Hybrid-JTE with implant dose of 1.8×10^{13}cm^{-2} show very similar behavior as in the case of the lower dose (1.3×10^{13}cm^{-2}) implanted structure as shown in Fig. 11. The MFZ-JTE and the Hybrid-JTE should provide similar blocking behaviors when implanted at a high JTE dose. However, the reverse i-v characteristics for the MFZ-JTE exhibit snapbacks as shown in Fig. 12. This can be attributed to the narrow width of the MFZ-JTE. Fig. 13 shows microscope images of the MFZ-JTE and the Hybrid-JTE structures after the destructive measurement that provides a conductive path resulting in a snapback in the current-voltage characteristics. Most of the destructive failures occurred at the corner of the edge termination structure near the anode metal where the highest localized surface electric field is generated with resultant large avalanche breakdown currents. From Fig. 11, it is observed that 3 dies out of 32- Hybrid-JTE structures show snapbacks. Therefore, when using the Hybrid-JTE structure, it is favorable to design the JTE implant schedule targeting the total dose in between 1.3×10^{13}cm^{-2} and 1.8×10^{13}cm^{-2} (or activated charge between 9×10^{12}cm^{-2} and 1.25×10^{13}cm^{-2}) for the case of 4500V SiC devices. In conclusion, it is demonstrated that the Hybrid-JTE provides wide process latitude that cannot be accomplished by the stand-alone MFZ-JTE, SZ-JTE, or RA-JTE methods.

IV. Conclusion

Various edge termination techniques such as FFRs, SZ-JTE, RA-JTE, MFZ-JTE, and Hybrid-JTE were investigated for 4500V-rated SiC devices. PiN diodes with these edge termination structures were designed, fabricated, and characterized. It was experimentally demonstrated that the RA-JTE and the Hybrid-JTE provide a nearly ideal breakdown voltage with tight distribution across the wafer. In addition, wider range of JTE implant doses is permissible for achieving high breakdown voltages using the Hybrid-JTE. This edge termination technique can be applied to SiC devices for other ranges of breakdown voltages as well.

Acknowledgement

The authors would like to thank Dr. Anant Agarwal, and Dr. Pawel Gradzki for their encouragement. The authors acknowledge the fabrication of the devices by XFAB, TX, U.S.

References

[1] B. J. Baliga, *Fundamentals of Power Semiconductor Devices.* New York, NY: Springer, 2008, Chap. 3, pp. 91–155.

[2] E. V. Brunt, L. Cheng, M. O'Loughlin, C. Capell, C. Jonas, , K. Lam, J. Richmond, V. Pala, S. Ryu, S. T. Allen, A. A. Burk, J. W. Palmour, and C. Scozzie, "22 kV, 1 cm^2, 4H-SiC n-IGBTs with Improved Conductivity Modulation," in *Proc. Int. Symp. Power Semiconductor Devices ICs, 2014*, pp. 358–361.

[3] T. Hiyoshi, T. Hori, J. Suda, and T. Kimoto, "Simulation and experimental study on the junction termination structure for high-voltage 4H-SiC PiN diodes," *IEEE Trans. Electron Devices*, vol. 55, no. 8, pp. 1841–1846, Aug. 2008.

[4] J. H. Zhao, P. Alexandrov, and X. Li, "Demonstration of the first 10-kV 4H-SiC Schottky barrier diodes,'' *IEEE Electron Device Lett.*, vol. 24, no. 6, pp.402–404, June. 2003.

[5] R. Perez, N. Mestres, S. Blanque, D. Tournier, X. Jorda, P. Godignon, and R. Nipoti, "A highly effective edge termination design for SiC planar high power devices," in *Mat. Sci. Forum*, vol. 457–460, 2004, pp. 1253–1256.

[6] W. Sung, E. Van Brunt, B. J. Baliga, and A. Q. Huang, "A New Edge Termination Technique for High-Voltage Devices in 4H-SiC – Multiple-Floating-Zone Junction Termination Extension,'' *IEEE Electron Device Lett.*, vol. 32, no. 7, pp.880–882, July. 2011.

[7] G. Feng, J. Suda, and T. Kimoto, "Space-Modulated Junction Termination Extension for Ultrahigh- Voltage p-i-n Diodes in 4H-SiC,'' *IEEE Trans. Electron Devices*, vol. 59, no. 2, pp. 414–418, Feb. 2012.

[8] K. Kinoshita, T. Hatakeyama, O. Takikawa, A. Yahata, and T. Shinohe, "Guard ring assisted RESURF: A new termination structure providing stable and high breakdown voltages for SiC power devices," in *Proc. Int. Symp. Power Semicond. Devices ICs*, 2002, pp. 253-256.

[9] W. Sung and B. J. Baliga, "A Near Ideal Edge Termination Technique for 4500V 4H-SiC Devices: the Hybrid Junction Termination Extension (Hybrid-JTE),'' *IEEE Electron Device Lett.*, vol. 37, no.12, Dec. 2016. DOI: 10.1109/LED.2016.2623423

[10] A. Bolotnikov, P. Losee, P. Deeb, M. Wang, G. Dunne, J. Kretchmer, S. Arthur, and L. Stevanovic, "Design of Area-efficient, Robust and Reliable Junction Termination Extension in SiC Devices," in *Mat. Sci. Forum*, vol. 858, 2016, pp. 737-740.

[11] A. O. Konstantinov, Q. Wahab, N. Nordell and U. Lindefelt, "Study of Avalanche Breakdown and Impact Ionization in 4H Silicon Carbide," *Journal of Electronic Materials*, Vol. 27, No. 4, 1998, pp. 335-341.